

## Effect of chromium on magnetite formation

Maria do Carmo Rangel<sup>1</sup>

*Institute of Chemistry, Universidade Federal da Bahia, Salvador, Bahia 40 170-280, Brazil*

Renato Massami Sassaki and Fernando Galembeck

*Institute of Chemistry, Universidade Estadual de Campinas, Campinas,  
São Paulo 13 084-100, Brazil*

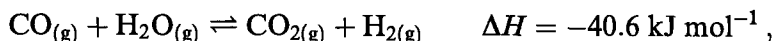
Received 14 March 1994; accepted 18 April 1995

Chromium-doped magnetite is the traditional catalyst used in the high temperature shift reaction in industrial processes. This work reports a method for preparing this solid, by heating chromium-doped iron(III)hydroxoacetates (IHA), prepared both by coprecipitation and by impregnation. This method provides the production of the catalyst in its active form avoiding the step of activation in industrial processes. It was noted that the presence of chromium affects magnetite formation as well as its characteristics. IHA containing chromium produces magnetite at higher temperature than does the pure IHA. Chromium-doped magnetites have higher surface areas, are less crystalline, have lower Fe(II)/Fe(III) ratios and are catalysts more active than those obtained from plain IHA. These effects depend on the preparation method of the precursor. It was also found that the impregnated sample is made of aggregates of a few crystals whereas the coprecipitate is made of smaller polycrystalline particles. In addition, the coprecipitation method leads to a more even distribution of chromium in solids. These observations are consistent with the best performance shown by the catalyst prepared by coprecipitation.

**Keywords:** magnetite formation; chromium-doped magnetite; HTS catalyst; iron(III)hydroxoacetate

### 1. Introduction

The water–gas shift reaction (WGSR) [1],



is often carried out in hydrogen and ammonia plants, to maximize hydrogen production from natural gas or naphtha feedstock, by ensuring that the carbon monoxide formed in the reforming process can be shifted to hydrogen and carbon dioxide production [1–3]. This reaction is also used in plants for the production of

<sup>1</sup> To whom correspondence should be addressed.

town gases to reduce the carbon monoxide contents to limits acceptable to local authorities [3] as well as in coal gasification [4,5]. Since the WGSR can take place whenever carbon monoxide and water are present, it may be an important step or side reaction in many other processes.

The WGSR is moderately exothermic and the forward reaction is favored by low temperatures and excess of steam; however, high temperatures are required to achieve rates suitable for commercial purposes. Therefore, when a process demands high-purity hydrogen (e.g. ammonia synthesis), the WGSR reaction should be performed in two steps, at different temperatures, using catalysts designed to operate in each stage. At high temperatures (300–400°C) it is carried out on iron–chromium spinel catalysts, whereas copper-based catalysts are used at lower temperatures (200–250°C) to remove carbon monoxide in thermodynamically favorable conditions [1–3].

The ferrochrome catalysts, usually used in industrial processes [1–3], have the advantages of low cost, thermal stability, as well as the ability to support a considerable amount of impurities without poisoning. However, the commercial catalyst is available as hematite and must be reduced to magnetite, which is found to be the active form. This process is often performed *in situ* by using the process gas. In ammonia plants, it is a mixture of carbon monoxide, carbon dioxide, nitrogen, hydrogen and methane. The reduction reaction is exothermic and should be carefully controlled by using water vapor, in order not to damage the catalyst and the reactor [2]. The reduction to metallic iron must be avoided since it may lead to carbon deposition and may catalyze undesirable reactions such as Fischer–Tropsch hydrocarbon synthesis [1]. Therefore, the development of ferrochrome catalyst in magnetite form may increase the process efficiency not only because of the energy saved but also due to the increase of the life of the catalyst.

Heating of iron(III)hydroxoacetate (IHA), a hydrated ferric oxyhydroxide, amorphous to X-rays, has proven a useful method to prepare magnetite [6]. This procedure may be a convenient way to produce chromium-doped magnetite, since it employs low temperatures (250–400°C) and yields the catalyst in its active form.

The production of chromium-doped magnetite by heating chromium-doped IHA prepared both by coprecipitation and impregnation is described in this work. The preparation method was related to the catalytic performance of the solids. The effect of chromium on IHA thermolysis was also investigated, in order to elucidate how chromium can affect the reactivity of IHA and the characteristics of the resulting magnetite.

In dealing with solid catalysts, it has been frequently noted that the preparation method of the solids can play a decisive role on the characteristics of the materials as well as on their activities [7,8]. It has also been noted that catalysts having the same X-ray structure may show different performances [9]. On the other hand, it is widely accepted that the reactivity of solids depends on the nature as well as on the concentration of lattice imperfections such as point defects, line defects and

impurities [10]. These can be generated throughout the catalyst preparation including aging or heat treatments which leads a freshly precipitated product from its initial amorphous phase to the final crystalline phase. By considering these aspects, it is important to elucidate which factors may determine the reactivity of IHA to produce magnetite.

## 2. Experimental

Reagents used were analytical grade.

The pure IHA sample was synthesized as follows: a 25% ammonium hydroxide solution was added to a 1 N iron nitrate solution under vigorous stirring. The gel of iron(III) hydroxide produced was washed six times with 600 ml of a 5% (w/v) ammonium acetate solution in order to promote acetate sorption in the gel and to remove nitrate ions. Then it was dried in an oven at 120°C (method 1).

IHA samples containing chromium were prepared by coprecipitation and impregnation methods. In the coprecipitation method (method 2) a 25% ammonium hydroxide solution was added to a mixture of 1 N iron nitrate and 0.4 N chromium nitrate solution under stirring. Then we proceeded as described in method 1. In the impregnation method (method 3) an iron(III) hydroxide colloidal dispersion was prepared by hydrolysis of a 1 N iron nitrate solution with ammonium hydroxide as in the method 1. Then it was mixed up with a 0.4 N chromium nitrate solution and mechanically stirred for 24 h. The sol was centrifuged and rinsed six times with a 5% (w/v) ammonium acetate solution as in the other methods.

The solids thus obtained were heated under nitrogen in the temperature range of 150–400°C, for 2 h.

To determine iron content, the materials were dissolved in 18% aqueous hydrochloric acid under reflux and titrated with standard potassium dichromate solution. Prior to total iron determination the samples were reduced with tin dichloride [11]. Chromium contents were determined by adding ammonium iron(II) sulfate to a solution of  $\text{Cr}^{3+}$  ions, previously oxidized to chromate. Fe(II) was titrated with standard potassium dichromate solution [12]. Carbon elemental analysis were carried out with a LECO 761-100 instrument.

Surface area measurements were made using the BET nitrogen adsorption method in a CG-2000 instrument. X-ray diffractograms were taken at room temperature, with a Philips PW 1130 instrument employing  $\text{Co K}\alpha$  radiation. Infrared spectra in the 4000–200  $\text{cm}^{-1}$  range were recorded in a model 1430 Perkin-Elmer spectrometer using cesium iodide discs.

Thermal analysis (DSC and TG) were performed in a model 9900 Du Pont apparatus at a heating rate of 10°C/min, under nitrogen atmosphere (100 ml/min).

Transmission electron micrographs were obtained in a Zeiss CEM-902 microscope. Powdered samples were dispersed in isopropanol and dropped on parlodion-carbon coated copper grids. Image acquisition was made either on SO-163 Kodak

film or using a SIT camera, in which case image processing was done in the microscope computer, using cem20 and ibas20 softwares.

The catalytic activity of the solids was measured in a fixed bed microreactor consisting of a stainless tube, using a gas composition around 8.1% CO, 5.3% CO<sub>2</sub>, 47.8% H<sub>2</sub>, 38.4% N<sub>2</sub> and 0.2% CH<sub>4</sub> and a steam/gas = 0.6. The volume of the catalyst taken in each experiment was 0.2 cm<sup>3</sup> of powder within -250 and +325 mesh size. All experiments were carried out under isothermal condition (370°C) and at atmospheric pressure providing that there is no diffusion effect. The reaction products were analysed by on line gas chromatography, using a CG-35 instrument. A commercial catalyst was also used to compare the catalytic performance of the samples prepared. After each experiment, the Fe(II)/Fe(III) ratio was measured to follow the iron reduction under the reactional atmosphere.

### 3. Results

#### 3.1. CHEMICAL ANALYSIS

The results of carbon, iron and chromium determinations in IHA samples are presented in table 1.

The acetate/Fe molar ratio has the same value in all samples, which means that acetate sorption does not depend on the chromium content nor on the preparation method. The Fe/Cr ratio is higher in solids prepared by impregnation, but the difference was not significant.

When the IHA samples were heated under nitrogen, they changed from brown to black and became magnetic. The Fe(II)/Fe(III) ratio increased with the heating temperature as shown in fig. 1. The solid exempt of chromium achieved a value (0.47) near to the stoichiometric value of magnetite (0.5) but the samples containing chromium did not. We may thus conclude that chromium decreases the efficiency of reduction of Fe<sup>3+</sup> to Fe<sup>2+</sup> ions. At higher temperatures, the materials prepared by impregnation showed the lowest values for the Fe(III)/Fe(II) ratio, showing that the reduction of Fe<sup>3+</sup> ions depends on the method of IHA preparation.

Table 1

Elemental analysis results of IHA and of chromium-doped IHA. W sample: plain IHA (prepared by method 1); P sample: chromium-doped IHA (method 2); I sample: chromium-doped IHA (method 3)

Sample	%Fe (±0.2)	%C (±0.1)	%Cr (±0.2)	Acetate/Fe molar ratio (±0.2)	Fe/Cr molar ratio (±0.2)
W	43.5	9.4	—	0.5	—
P	40.5	9.2	5.5	0.5	7.3
I	43.8	9.6	5.2	0.5	7.8

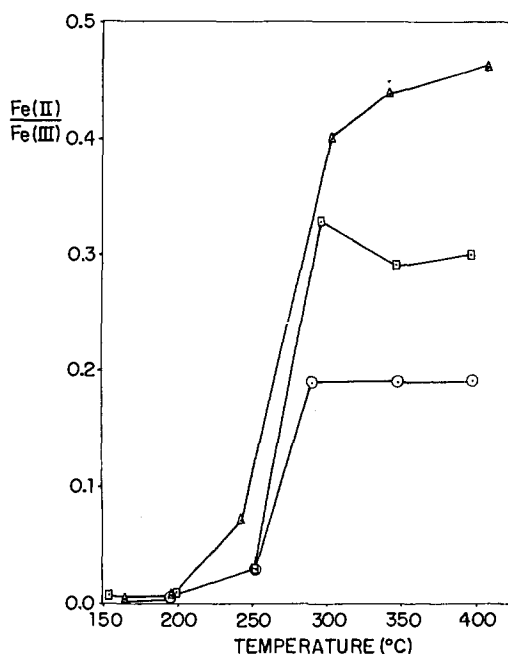


Fig. 1. Fe(II)/Fe(III) ratio in IHA and in chromium-doped IHA as a function of heating temperature. (△) IHA exempt of chromium (prepared by method 1); (□) chromium-doped IHA (method 2); (○) chromium-doped IHA (method 3).

As samples were heated, carbon contents decreased as shown in table 2. At 400°C, they achieved values of about 1%, which is a convenient amount of carbon for HTS catalysts, in order to aid pelletization, as it does in commercial formulations [13].

### 3.2. X-RAY DIFFRACTOGRAMS

X-ray diffractograms were taken on IHA and on chromium-doped IHA as a function of temperature.

Fig. 2 shows the diffractograms of solids exempt of chromium. Samples heated at temperatures below 200°C, display only an amorphous halo; at 250°C diffuse lines appear and become narrower and more intense as the temperature increases.

On the other hand, the diffractograms of the chromium-doped IHA (fig. 3) show that these solids remain amorphous (to X-rays) up to 250°C. At 300°C, the samples show diffractograms with diffuse lines which become narrower and more intense at higher temperatures. The lines displayed by samples prepared by impregnation are more intense and narrower than those shown by solids obtained by coprecipitation (fig. 3).

At higher temperatures, all samples presented diffractograms with the pattern of magnetite [14]. From the interplanar spacings ( $d$ ), shown in table 3, we can see

Table 2

Carbon contents of iron(II)hydroxoacetate (IHA) after heating at several temperatures for 2 h under nitrogen. W sample: plain IHA (prepared by method 1); P sample: chromium-doped IHA (method 2); I sample: chromium-doped IHA (method 3)

Calcination temperature (°C)	%C ( $\pm 0.1$ )		
	W sample	P sample	I sample
160	7.6	8.6	8.8
180	7.2	7.8	8.2
250	3.2	6.6	6.4
300	0.9	3.3	2.4
350	0.6	0.8	1.6
400	0.6	0.9	1.3

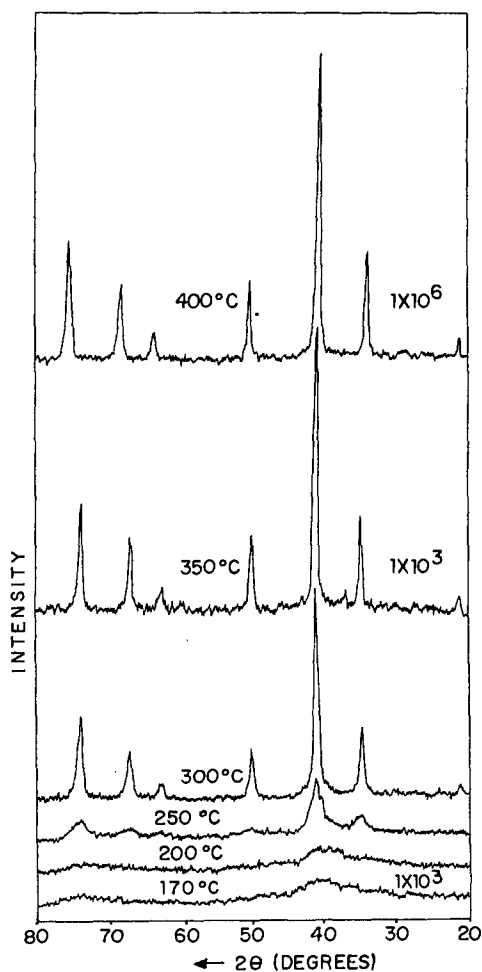


Fig. 2. X-ray diffractograms of IHA after heating at several temperatures for 2 h under nitrogen.

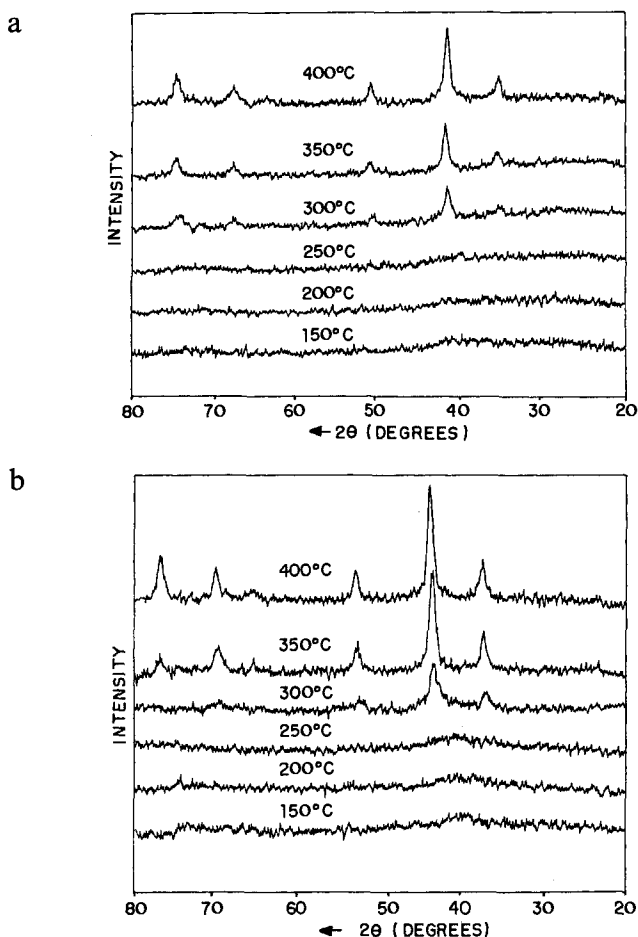


Fig. 3. X-ray diffractograms of chromium-doped IHA previously heated at several temperatures for 2 h under nitrogen. (a) Prepared by method 2; (b) prepared by method 3.

Table 3

Interplanar spacings ( $d$ ) of plain magnetite and chromium-doped magnetite. W sample: plain magnetite (method 1); P sample: chromium-doped magnetite (method 2); I sample: chromium-doped magnetite (method 3)

$hkl$	ASTM card No. 19269	$d$ (Å)		
		W sample	P sample	I sample
220	2.996	2.958	2.934	2.933
311	2.530	2.536	2.525	2.525
400	2.096	2.097	2.089	2.093
422	1.712	1.712	—	—
333/511	1.614	1.613	1.605	1.608
440	1.483	1.481	1.473	1.477

that chromium entered the magnetite lattice under the experimental conditions used in the sample preparation. A second phase (e.g. chromium oxide) was not detected by X-ray diffraction.

By comparing the diffractograms shown in figs. 2 and 3 we can see that the solids without chromium are more crystalline than the chromium-doped samples. Therefore, chromium retards the magnetite crystallization. From the results of fig. 3 we can also conclude that this effect depends on the method used for preparing the chromium-doped IHA.

### 3.3. INFRARED SPECTRA

The infrared spectra of pure IHA and chromium-doped IHA are shown in fig. 4. The presence of acetate in the solids was confirmed by the absorption bands at  $1550$  and  $1430\text{ cm}^{-1}$  [15]. The spectra also show bands at  $3400$  and  $1350\text{ cm}^{-1}$ , assigned to hydroxyl and nitrate groups respectively [16,17] beyond the broad Fe–O absorption band below  $800\text{ cm}^{-1}$  [18].

Fig. 5 shows the spectra of IHA samples previously heated at  $400^\circ\text{C}$  under nitrogen for 2 h. The spectrum of the solid without chromium shows bands at  $580$  and  $370\text{ cm}^{-1}$ , which are typical of magnetite [19]. In the spectrum of the chromium-doped samples these bands become broader, probably due to the incorporation of  $\text{Cr}^{3+}$  ions into the magnetite lattice, causing lattice distortion. The chromia characteristics bands [19] as well as the typical bands of chromates [20] were not detected.

### 3.4. SURFACE AREA MEASUREMENT

Table 4 shows the surface area of IHA and of chromium-doped IHA previously heated under nitrogen at  $400^\circ\text{C}$  for 2 h. The results show that surface areas of heated chromium-IHA are much larger than these of heated plain IHA, this effect being greater in the samples produced by coprecipitation. It means that chromium prevents pore closure or sintering or both, depending on the preparation method of the precursor.

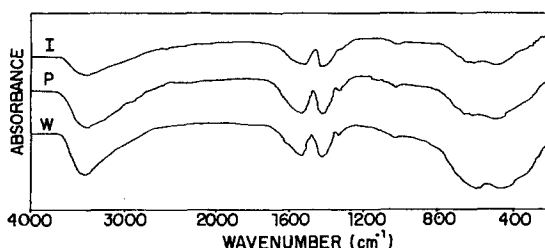


Fig. 4. Infrared spectra of IHA and of chromium-doped IHA. W sample: IHA exempt of chromium (prepared by method 1); P sample: chromium-doped IHA (method 2); I sample: chromium-doped IHA (method 3).



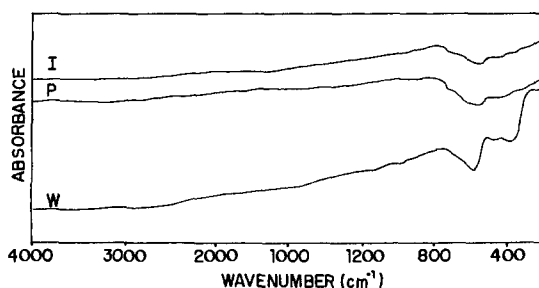


Fig. 5. Infrared spectra of IHA and of chromium-doped IHA, after heating at 400°C for 2 h under nitrogen. W sample: IHA exempt of chromium (prepared by method 1); P sample: chromium-doped IHA (method 2); I sample: chromium-doped IHA (method 3).

### 3.5. THERMAL ANALYSIS

Thermal analysis was performed on IHA samples to follow the magnetite production. The results are shown in fig. 6.

All thermograms shows an endothermic peak below 200°C. Since the amount of Fe(II) in the solids heated in this temperature range is negligible (fig. 1), this peak may be assigned to the loss of volatile components with consequent generation of pores in the solids.

The DSC curves changed with the presence of chromium. The thermogram of the IHA exempt of chromium shows two exothermic peaks at temperatures higher than 200°C, whereas there is only one endothermic peak at 318°C in the thermograms of chromium-IHA samples. From fig. 1, we can see that most of Fe(II) is formed at temperatures above 200°C in plain IHA samples and above 250°C in chromium-doped samples. Therefore, we may associate these peaks with magnetite formation. As IHA decomposition involves magnetite formation as well as acetone, acetic acid, carbon monoxide and carbon monoxide release [21], the form of this peak depends on the extension of each process. Since the enthalpy of magnetite formation is negative ( $-8971.5 \text{ kJ mol}^{-1}$ ) and crystallization processes are also exothermic, we can expect a more exothermic peak in the thermogram of the plain magnetite sample which was more crystalline and had the highest Fe(II)/Fe(III) ratio. On the other hand, in the chromium-doped solids, both magnetite formation

Table 4

Surface area (Sg) of IHA and of chromium-doped IHA previously heated at 400°C under nitrogen for 2 h. W sample: IHA without chromium (prepared by method 1); P sample: chromium-doped IHA (method 2); I sample: chromium-doped IHA (method 3)

Sample	Sg (m <sup>2</sup> g <sup>-1</sup> )
W	33
P	140
I	100

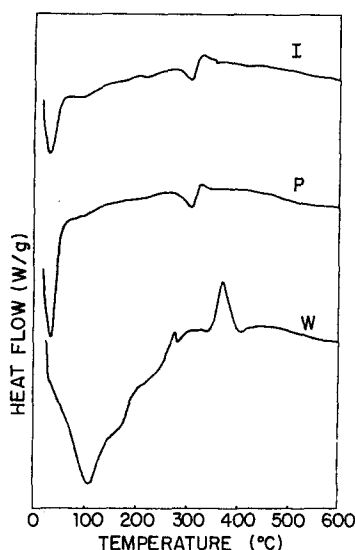


Fig. 6. DSC thermograms of IHA and of chromium-doped IHA samples. W sample: IHA without chromium; P sample: chromium-doped IHA prepared by method 2; I sample: chromium-doped IHA prepared by method 1.

and its crystallization were delayed and the thermograms show an endothermic peak.

We can then conclude that magnetite formation begins at about 207°C in the case of pure IHA, whereas it begins at about 287°C in the chromium-doped samples.

The exothermic peak at 450°C, assigned to the transformation of amorphous chromium hydroxide to crystalline chromium oxide [22], was not detected.

### 3.6. TRANSMISSION ELECTRON MICROSCOPE

The morphologies of the impregnated and coprecipitated chromium-doped magnetites are different, as shown in fig. 7. The impregnated sample is made of aggregates of a few crystals, with smooth surfaces; the corresponding diffractograms present a few, intense reflections. On the other hand, the coprecipitated sample is made of many small particles, in which diffractogram two features are discernible: complete rings together with isolated reflection spots. This is consistent with the coexistence of randomly oriented, small crystals together with a few larger crystals. The reflections observed are assigned to  $\alpha$ -Fe<sub>2</sub>O<sub>3</sub>, Cr<sub>2</sub>O<sub>3</sub> or solid solutions of these.  $\alpha$ -Fe<sub>2</sub>O<sub>3</sub> is probably formed due to oxidation of the fine magnetite particles, under air. Interplanar spacings of hematite and chromia are coincident, within a few hundredths of angstrom, which is within the precision of our electron diffraction measurements.

Fig. 8 shows dark-field pictures of the same aggregate of the impregnated sam-

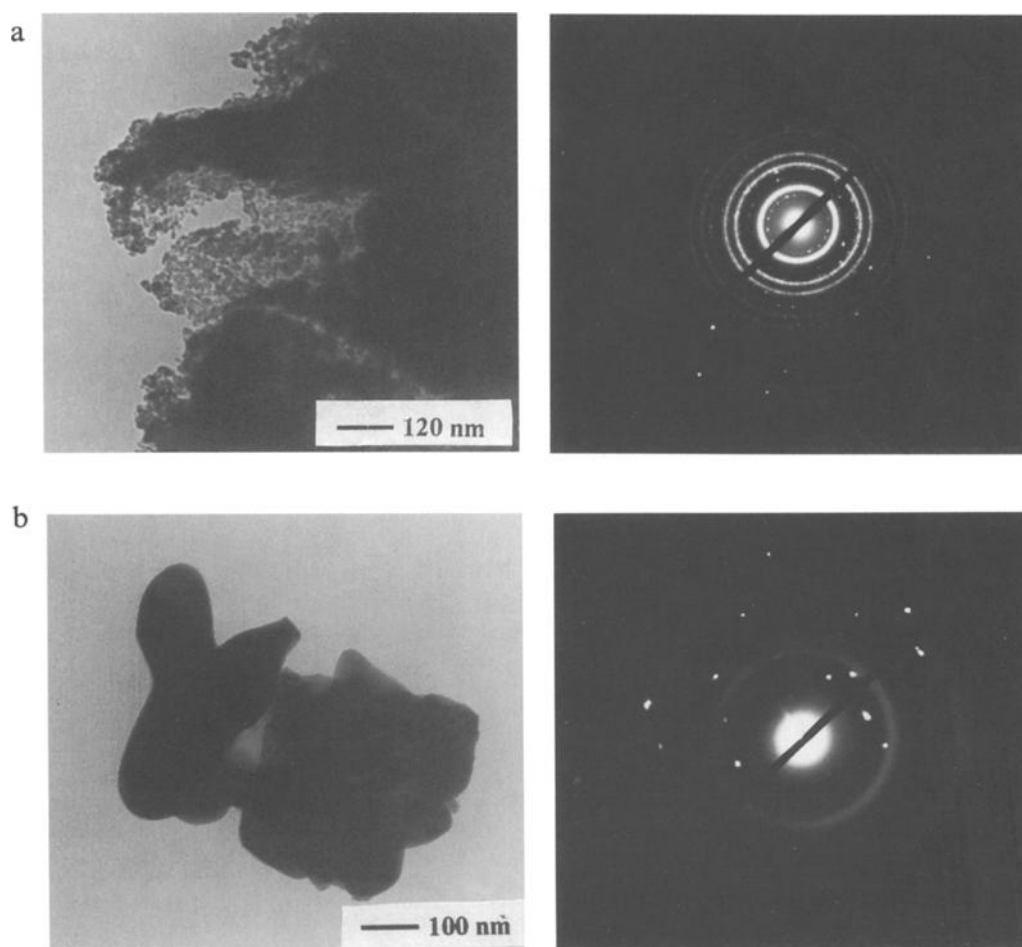


Fig. 7. Clear-field transmission micrographs of chromium-doped IHA samples heated at 400°C (a) prepared by method 2 (P sample); (b) prepared by method 3 (I sample).

ple, seen in fig. 7. The dark-field pictures were obtained using different diffracted beams, selected with the objective diaphragm. Clear spots extend throughout large areas, showing that single crystal dimensions are in excess of 2  $\mu\text{m}$ . The formation of uniformly oriented terraces is also clear; rounded-off crystal perimeters can be seen, which point to the existence of large-index planes, at the crystal surfaces.

A further, important feature of the impregnated sample may be observed in fig. 9, which presents two elemental distribution images (for Cr and Fe), obtained using ELSI. In the same figure, two other micrographs are presented, both obtained using filtered electrons (at 0 and 250 eV energy loss). The latter gives a view of the individual particles and domains within the aggregate. Chromium and iron are not distributed evenly throughout the sample and distinct domains are seen, in the size range of 100–200 nm.

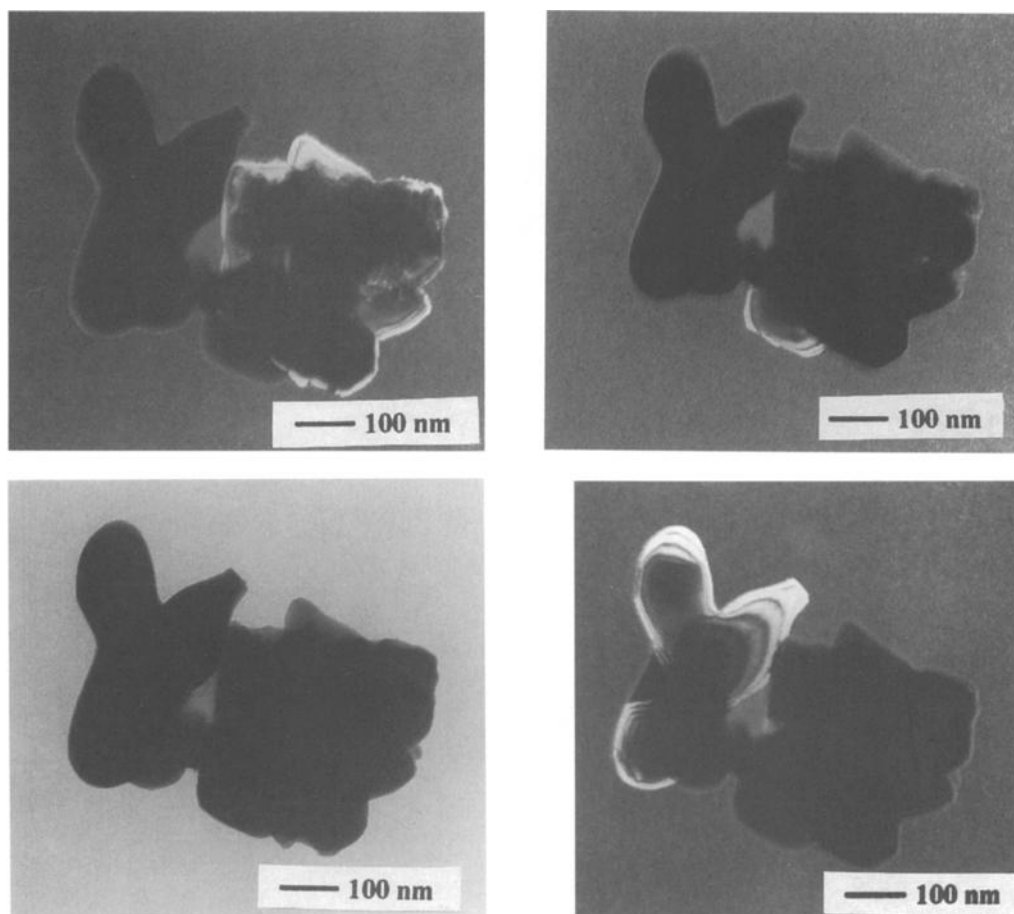


Fig. 8. Clear- and dark-field transmission micrographs of the same aggregate from sample I, seen in fig. 7. Each of the dark-field images was obtained using a different diffracted spot.

Cr and Fe elemental distributions do overlap much better in the coprecipitated sample, as seen in fig. 10. There are some contrast differences in some areas of both pictures, but these are limited to features in the 10 nm size range. This means that the elements are more evenly distributed than in the sample prepared by impregnation.

### 3.7. CATALYTIC ACTIVITY MEASUREMENT

The activity of the catalysts towards the HTS reaction are shown in table 5. The Fe(II)/Fe(III) ratio of fresh and used catalysts is also presented in order to evaluate the magnetite stabilization under the reactional atmosphere.

It was noted that all solids catalyze the HTS reaction; as expected, the chromium-doped samples are the most active and the catalytic performance chan-

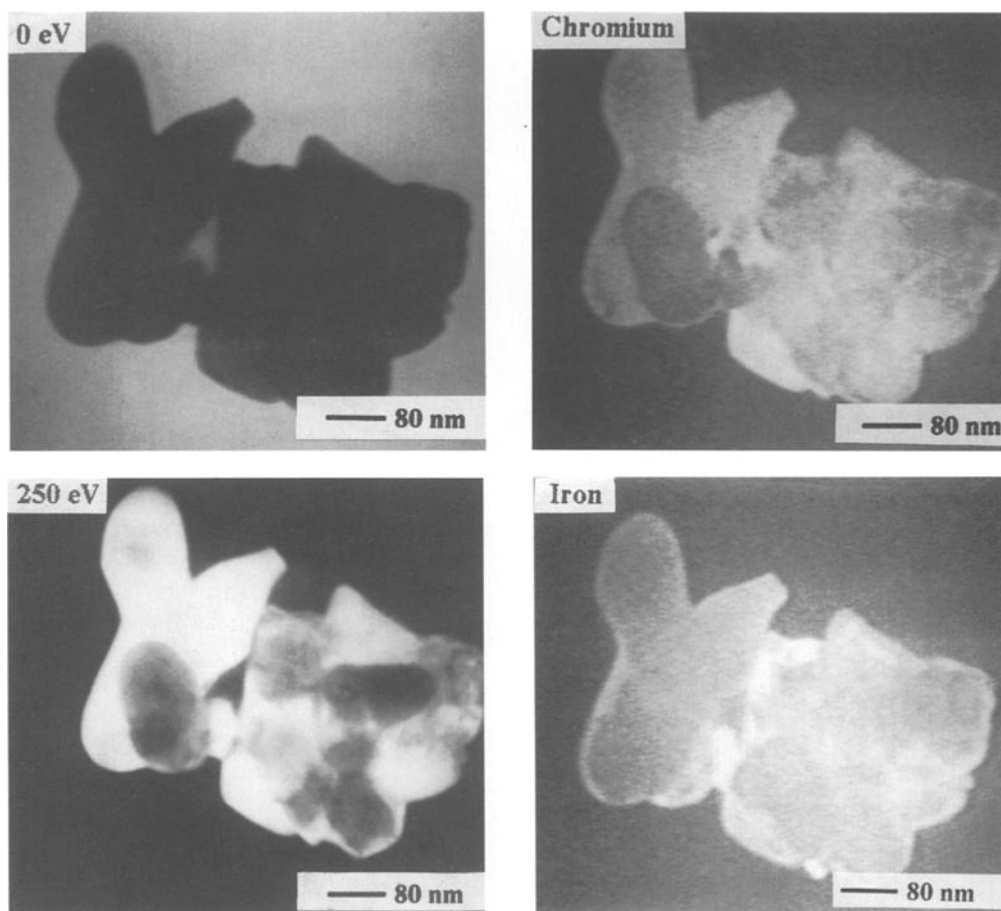


Fig. 9. Monochromatic pictures of the same aggregate of sample I, seen in fig. 7, together with chromium and iron elemental distribution images. Clear areas are element-rich. The 250 eV picture helps viewing the individual domains, within the aggregates.

ged with the preparation method. The coprecipitated sample was the most efficient, showing an activity higher than a chromium-doped commercial catalyst ( $11 \times 10^{-4} \text{ mol g}^{-1} \text{ h}^{-1}$ ).

By comparing the Fe(II)/Fe(III) ratio of fresh and used catalysts it can be seen that magnetite underwent further reduction under the reactional atmosphere; again, this process is delayed by chromium and depends on the preparation method of the precursor.

#### 4. Discussion

Chromium-doped magnetite was produced by heating IHA under nitrogen. By

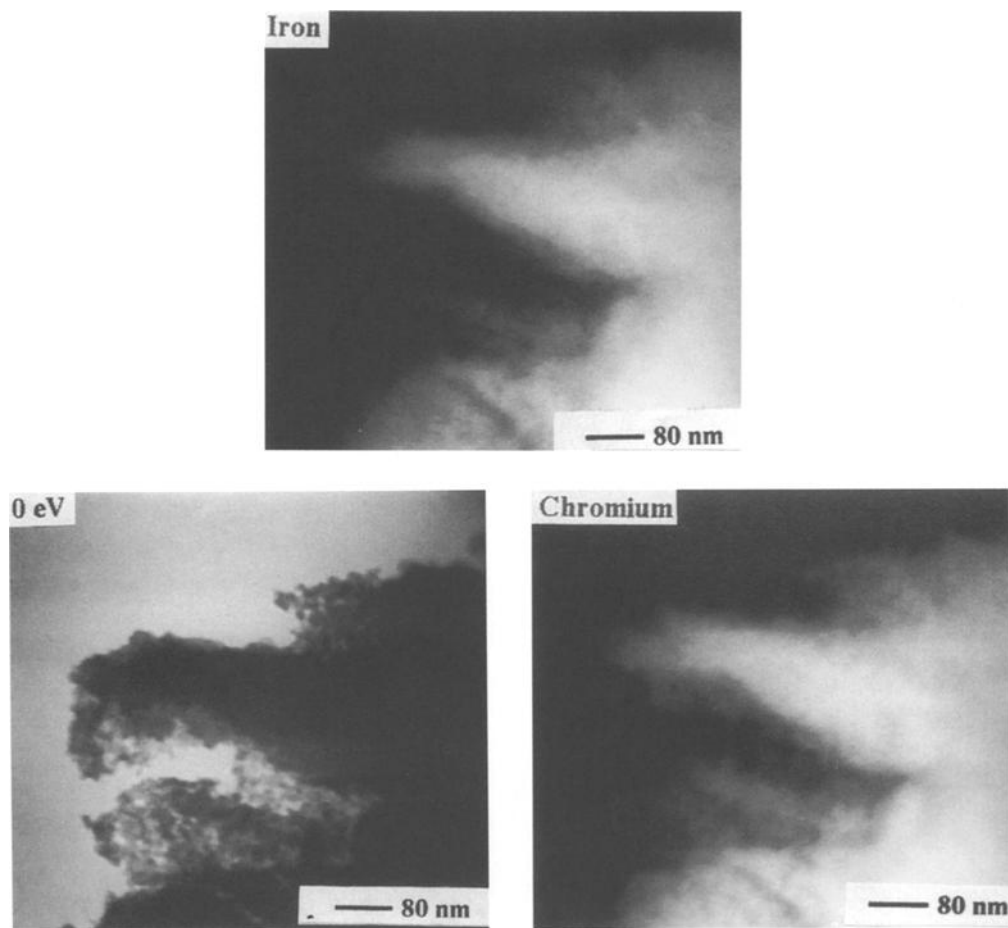


Fig. 10. Clear-field image and elemental distribution in sample P.

Table 5

Catalytic activity ( $a$ ) of plain and chromium-doped magnetite towards the HTS reaction. W sample: plain magnetite (method 1); P sample: chromium-doped magnetite (method 2); I sample: chromium-doped magnetite (method 3)

Sample	$a \times 10^4$ (mol g <sup>-1</sup> h <sup>-1</sup> )	Fe(II)/Fe(III)	
		fresh catalyst	used catalyst
W	5.8	0.47	0.48
P	11	0.19	0.37
I	15	0.30	0.41

using impregnation and coprecipitation methods, solids with different characteristics were prepared. The chromium-doped IHA obtained by impregnation yielded, upon heating, a magnetite which is more crystalline and has a lower surface area than the solids produced by heating the chromium-doped coprecipitate. Furthermore, the samples prepared by impregnation showed the lowest value of the Fe(II)/Fe(III) ratio, after heating.

The presence of chromium affects magnetite formation as well as its characteristics. The DSC thermogram of pure IHA shows that magnetite formation begins at about 207°C, whereas in the chromium-promoted samples it begins at about 287°C. So, chromium delays magnetite formation, a conclusion which is confirmed by the values of Fe(II)/Fe(III) ratio, as well as by the X-ray results. Chromium-doped magnetites are also less crystalline and they have higher surface areas and lower Fe(II)/Fe(III) ratios than the pure magnetite, also obtained by IHA thermolysis.

We may conclude that chromium modifies the reactivity of IHA, as well as its sintering and crystallization behavior.

As far as the precipitation of iron and chromium hydroxides is concerned, it has been pointed out by several authors [23–28] that  $\text{Fe}^{3+}$  and  $\text{Cr}^{3+}$  undergo hydrolysis and further polymerization in aqueous medium, as the pH increases. At low pHs, each cation exists as a simple aquo-ion and at high pHs it precipitates as the hydroxide or as hydroxosalts. Both  $\text{Fe}^{3+}$  and  $\text{Cr}^{3+}$  ions form octahedral complexes. As the  $\text{Fe}^{3+}$  cation ( $3d^5$ ) exhibits no crystal field stabilization in octahedral symmetry, the rates of hydrolysis and of polymerization are higher than those of the  $\text{Cr}^{3+}$  ion ( $3d^3$ ) which shows a high crystal field stabilization in the same symmetry. The most crystal field-stabilized ion would be the least hydrolyzed since  $\text{OH}^-$  presumably produces a weaker field than  $\text{H}_2\text{O}$ . On the other hand, lation reaction rates must be slowed down as the crystal field stabilization increases since it implies a decrease of the reactivity of the cation towards ligand exchange. In agreement, the rate of dimerization of the  $[\text{Fe}(\text{OH})(\text{OH}_2)_5]^{2+}$  ion is  $k = 450 \text{ M}^{-1} \text{ s}^{-1}$  at 25°C, whereas the rate of dimerization of the  $[\text{Cr}(\text{OH})(\text{OH}_2)(\text{C}_2\text{O}_4)_2]^{2-}$  is  $k = 10^{-5} \text{ M}^{-1} \text{ s}^{-1}$  [23]. Therefore it is expected that the  $\text{Fe}^{3+}$  ion forms chains longer than the  $\text{Cr}^{3+}$  ion as a result of polymerization following hydrolysis.

When iron and chromium hydroxides are coprecipitated, a mixed hydroxide is formed. The solid hydroxide is believed to be built of chains consisting of  $\text{Fe}^{3+}$  and  $\text{Cr}^{3+}$  ions in an octahedral array with acetate linked to metal ions. As the two cations have about the same radii ( $\text{Fe}^{3+} = 0.64 \text{ \AA}$ ;  $\text{Cr}^{3+} = 0.63 \text{ \AA}$ ) the  $\text{Cr}^{3+}$  ion is not expected to increase the strain in the polymerized structure but rather to yield a more inert chain due to the high crystal field stabilization of  $\text{Cr}^{3+}$  in the octahedral symmetry.

On the other hand, in the samples prepared by impregnation, a mixed chain is not expected: the iron(III)hydroxoacetate is formed first, grows to a greater extent and chromium impregnation is then done on grown-up, already coalesced particles.

The mixed hydroxide is converted into chromium-doped magnetite upon heating. As the chains are more inert due to the presence of chromium, the species will have a greater difficulty to react, to sinter or to crystallize. Enough mobility for the reaction of magnetite formation to proceed is only achieved upon heating at higher temperatures, as shown by DSC curves, X-ray diffractograms, surface areas as well as by Fe(II) determinations. However, during the spinel formation, the reduction of  $\text{Fe}^{3+}$  ions is delayed due to the fact that  $\text{Cr}^{3+}$  having an octahedral site preference substitutes into the available octahedral sites in the magnetite lattice, thus preventing the formation of the  $\text{Fe}^{2+}$  ions.

In impregnated samples, chromium is probably sorbed on IHA particles and the same effects described for the coprecipitated samples are also expected. The presence of this dopant in the magnetite lattice is confirmed by the values of interplanar spacings.

From the transmission electron microscopy results, we found that the preparation method of the precursor leads to important differences in the sample morphologies. Particles prepared by impregnation, in which iron(III)hydroxoacetate is formed first, grow larger than the mixed-cation particles. Impregnation is thus done on grown-up, coalesced particles; chromium accumulates in some areas, leading to uneven element distribution on larger domains, whereas in the coprecipitated samples, chromium is precipitated together with iron and the morphological changes on the mixed oxide particles are slower, preventing their growth. As a result, impregnated samples are made of bigger particles, as compared to mixed-cation particles, and have an uneven element distribution on larger domains. This may be understood considering the same basic kinetic argument already described: ligand exchange around Fe ions is much faster than around Cr ions.

A  $\text{Cr}_2\text{O}_3$  phase was not detected in solids by infrared, X-ray and electron diffraction or DSC techniques. It has been known [29] that chromia can occur in various degrees of hydration, either amorphous or crystalline, mesoporous or microporous, with various surface concentrations of  $\text{Cr}^{3+}$  and  $\text{O}^{2-}$  and with various degrees of excess oxygen. Because of this excess, it is necessary first to heat chromia under hydrogen to about  $300^\circ\text{C}$ , during catalyst activation. Our experimental evidence does not preclude the existence of chromia and this was confirmed by the transmission electron microscopy experiments in which no plain chromium phase was found.

The most active catalyst was the sample prepared by coprecipitation. It can be assigned to its larger surface area, its higher Fe(II)/Fe(III) molar ratio and its more homogeneous chromium distribution. This last feature can be particularly important in delaying sintering during the life of the catalyst, thus avoiding the decay of activity which is frequently noted in industrial processes. It has been reported [30] that activity is lost due to a gradual loss of surface area of the catalyst, under the reactional conditions.

The chromium-doped magnetite prepared by coprecipitation showed a better performance than did the commercial catalyst. It means that the method described



in this paper may be a convenient way to prepare the HTS catalysts for industrial purposes.

## 5. Conclusions

Heating of iron(III)hydroxoacetate (IHA) doped with chromium has proven a convenient method to prepare chromium-doped magnetite. The presence of chromium delays both magnetite formation and its crystallization and sintering; these effects depend on the preparation method of the precursor. It was noted that the impregnated sample is made of aggregates of a few crystals, whereas the coprecipitation is made of aggregates of smaller crystalline particles. Furthermore, the coprecipitation method leads to a more even distribution of chromium in the solids. Under the experimental conditions used in the sample preparation, chromium enters the magnetite lattice leading to lower values of the Fe(II)/Fe(III) ratio, in this solid.

Although we have not detected a chromia phase, usually found in the industrial ferrochrome catalysts [3] often employed in the high temperature shift reaction, the chromium-doped sample prepared by coprecipitation showed an activity higher than the commercial catalyst. Therefore, the methods used are a convenient and effective way to prepare these catalysts, in its active form.

## Acknowledgement

The authors acknowledge to Marluce Oliveira da Guarda Souza for her help in the experiments of catalytic activity. MCR acknowledges a PICD-CAPES graduate fellowship. This work was supported by grants from FAPESP, CNPq and FINEP.

## References

- [1] J.S. Campbell, P. Craven and P.W. Young, in: *Catalysis Handbook* (Wolfe, London, 1970) p. 97.
- [2] C.N. Satterfield, in: *Heterogeneous Catalysis in Practice* (McGraw-Hill, New York, 1980) p. 292.
- [3] H. Bohlbro, in: *An Investigation on the Kinetics of the Conversions of Carbon Monoxide with Water Vapor over Iron Oxide Based Catalysts* (The Haldor Topsøe Laboratory, Vedback, 1969) p. 9.
- [4] M.R. Appell et al., *Chemical Industry* (1982) 1703.
- [5] N.N. Lebedev, in: *Chemistry and Technology of Basic Organic and Petrochemical Synthesis* (Mir, Moscow, 1984) p. 561.
- [6] E.A. Pinheiro, P.P. Abreu Fo., F. Galembeck, H. Vargas and E.C. Silva, *Langmuir* 5 (1987) 445.

- [7] J.H. De Boer, in: *Proc. 4th Int. Symp. on the Reactivity of Solids* (Elsevier, Amsterdam, 1961).
- [8] M. Shimokawabe, R. Furuichi and T. Ishii, *Thermochim. Acta* 21 (1977) 377.
- [9] R. Furuichi, N. Sato and G. Okamoto, *Chimia* 23 (1969) 455.
- [10] N.B. Hannay, in: *Solid State Chemistry* (Prentice Hall, Englewood Cliffs, 1957) p. 100.
- [11] A.I. Vogel, in: *Quantitative Inorganic Analysis* (Longman, London, 1961) p. 309.
- [12] H. Bennet and R.A. Reed, in: *Chemical Methods of Silicate Analysis. A Handbook* (Academic Press, London, 1971) p. 129.
- [13] A. Styles, in: *Catalyst Manufacture. Laboratory and Commercial Preparations* (Dekker, New York, 1983) p. 117.
- [14] ASTM card No. 19 269.
- [15] R. Silverstein, G.C. Bassler and T.C. Morrill, in: *Spectrometry Identification of Organic Compounds* (Wiley, New York) p. 121.
- [16] J.D. Russell, *Clay Minerals* 14 (1979) 109.
- [17] R.A. Niquist and R.O. Kagel, in: *Infrared Spectra of Inorganic Compounds* (Academic Press, Orlando, 1971) p. 3.
- [18] U. Schwertmann and W.R. Fischer, *Geoderma* 10 (1973) 237.
- [19] N.T. McDevitt and W.L. Baun, *Spectrochim. Acta* 20 (1964) 799.
- [20] J.A. Campbell, *Spectrochim. Acta* 21 (1965) 1333.
- [21] P.P. de Abreu Filho, E.A. Pinheiro and F. Galembeck, *React. Solids* 3 (1987) 241.
- [22] S.K. Bhattacharya, V.S. Ramachandran and J.C. Ghosh, *Adv. Catal.* 9 (1957) 114.
- [23] J.P. Punt, in: *Metal Ions in Aqueous Solution* (Benjamin, New York, 1965) pp. 45–54.
- [24] C.F. Baes Jr. and R.E. Mesmer, in: *The Hydrolysis of Cations* (Wiley, New York, 1976) pp. 211–219, 235, 266.
- [25] J. Burgess, in: *Metal Ions in Solution* (Wiley, New York, 1978) pp. 269–309.
- [26] J. Livage, M. Henry and C. Sanchez, *Progr. Sol. State Chem.* 8 (1988) 259.
- [27] H. Wendt, *Inorg. Chem.* 8 (1969) 1537.
- [28] M.A. Blesa and E. Matijetic, *Adv. Colloid Interf. Sci.* 29 (1989) 173.
- [29] R.L. Burwell Jr., A.B. Littlewood, M. Cardew, G. Pass and C.T.H. Stoddart, *J. Am. Chem. Soc.* 82 (1960) 6272.
- [30] G.C. Chinchin, R.H. Logan and M.S. Spencer, *Appl. Catal.* 12 (1984) 89.